Optical and Magneto-Optical Properties of Some Semiconductors

Optical and Magneto-Optical Properties of Some Semiconductors*

Yuichiro NISHINA, Kunihide TANAKA, Susumu KURITA, Masao YAMAMOTO, Takehito JIMBO, Noritaka KURODA and Tadao FUKUROI

(Received October 11, 1966)

Synopsis

This article reviews our works on the visible and infrared studies of semiconductors during past two years. The problems treated here are concerned mainly with the experimental determination of the electronic band parameters in Ge, PbTe, PbSe, GaSe, InSb and $(HgTe)_{1-x}(CdTe)_x$ (x=0, 0.15) in terms of the effective mass approximation. The measurements on most of these substances were carried out with respect to their intraband or interband magneto-absorption and the rotatory dispersion at several values of temperature in the range from 1.77°K to 300°K. The far-infrared measurements on GaSe, GaS and HgTe showed the absorption peaks associated with their lattice vibrations. Three kinds of magnets were used for producing the magnetic field in the above experiments: 1) Bitter solenoid of Helmholtz type with the maximum magnetic field of 39 kgauss, 2) Superconducting magnet made particularly convenient for the magneto-optical measurements and 3) Pulse magnet with its maximum field of 201 kgauss by means of condenser discharge.

1. Introduction

Among the various methods of investigating the electronic properties of semiconductors, the optical measurements are known to give the following informations on their electronic band structures:

(1) Energy gap between the extremes of the valence band and of the conduction band.
(2) Effective masses of electron and hole at or near the band extremes.
(3) Symmetry of the band structure and, hence, the selection rule for the electronic transition from a filled state to an empty one.
(4) Effect of spin-orbit coupling and the effective g-factor.
(5) Exciton effect.
(6) Relaxation time for the scattering of electron and hole.

It is almost impossible for conventional transport measurements to give significant information on all of the above parameters for the electronic band structure of a semiconductor. Furthermore, it is often difficult at high temperatures to separate the quantity in (2) from that in (6) by the observed values of mobilities of electrons and/or holes which usually give the ratios of (2) to (6).

The optical measurements over the wide range of wavelength, on the other

* The **1282nd** report of the Research Institute for Iron, Steel and Other Metals.

hand, can give the quantities (2) and (6) separately, because they deal mainly with the anomalous dispersion associated with optical resonances. Moreover, with the use of a strong magnetic field, the optical measurements enable us to find the numerical values of (1) and (2) with the accuracy which has never been equalled by the transport measurements.[1] Also the measurement of the rotatory dispersion is known to be a powerful means for investigating the effect in (4). The experimental results to be described here give some examples in favor of the above arguments.

The optical experiments reported here were carried out with our particular attention to the absorption with or without the external magnetic field and the rotatory dispersion of the incident radiation due to the field. In terms of the phenomenological complex conductivity tensor,

$$\overleftrightarrow{\sigma} = \begin{pmatrix} \sigma_{xx} & \sigma_{xy} & \sigma_{xz} \\ \sigma_{yx} & \sigma_{yy} & \sigma_{yz} \\ \sigma_{zx} & \sigma_{zy} & \sigma_{zz} \end{pmatrix}, \tag{1}$$

the absorption measurements can give the diagonal element of this tensor as a function of the wavelength and the external field. In the crystals of cubic symmetry the non-diagonal components of this tensor become zero in the absence of the magnetic field. An external field, H_0, applied in the z-direction, however, causes the change in the tensor elements as follows:

$$\begin{aligned} &\sigma_{xy} = -\sigma_{yx} \neq 0 \\ &\sigma_{xx}(H_0) - \sigma_{zz}(H_0) \neq 0 \\ &\sigma_{yy}(H_0) - \sigma_{zz}(H_0) \neq 0 \\ &\sigma_{zz}(0) = \sigma_{zz}(H_0) . \end{aligned} \tag{2}$$

In this configuration of the external field, the plane of polarization of the incident radiation rotates as the electromagnetic wave propagates through the solid. The wavelength dependence of such rotation is called the rotatory dispersion which can occur in the following two cases:

(1) $\vec{H}_0 // \vec{S}$, where $\vec{S}$ is the Poynting vector of the electromagnetic field. The rotation in this case is called the Faraday effect.

(2) $\vec{H}_0 \perp \vec{S}$ and $\vec{E} = \vec{E}_{//} + \vec{E}_{\perp}$, where $\vec{E}$ is the electric vector of the wave which consists of the two components, i.e. parallel (//) and perpendicular ($\perp$) to $\vec{H}_0$. The birefringence induced by H_0 is called the Voigt effect.

If the external field is weak such that

(1) For a review of magneto-optical measurements see for example B. Lax, "Proc. International School of Physics, Course XXII, Varenna, Italy, July 1961", ed. by R.A. Smith (Academic Press, N.Y. 1963), p. 240.

$$\sigma_{xy}(H_0) \ll \sigma_{xx}(H_0), \qquad \sigma_{xx}(H_0) - \sigma_{zz}(H_0) \ll \sigma_{xx}(H_0),$$

the Faraday rotation angle, θ, and the Voigt phase shift, δ, for a unit distance in the z-direction can be approximately described by the conductivity tensor as follows,

$$\theta \equiv \frac{\omega}{2c}(n_- - n_+) \fallingdotseq \frac{2\pi}{nc} Re(\sigma_{xy}), \tag{3}$$

$$\delta \equiv \frac{\omega}{c}(n_{//} - n_{\perp}) \fallingdotseq \frac{2\pi}{nc} Im(\sigma_{xx} - \sigma_{zz}), \tag{4}$$

where n is the index of refraction, $+$, $-$, correspond to those for the circularly polarized waves of the $+$, $-$ senses and $//$, $\perp$ for the waves with the electric vectors parallel and perpendicular to the magnetic field, respectively.

The physical causes of our interest here in optical anomalies of semiconductors may be classified in the following three categories:

(1) Interband effects

If an incoming radiation has an energy sufficient to excite an electron from the valence band to the conduction band, the radiation will be absorbed as a consequence of the electronic excitation. Moreover, the external magnetic fields will give rise to the magnetic sublevels in both bands as they were originally explained by Landau.[2] Then the absorption spectrum will reveal the magnetic substructures near its fundamental absorption edge because of the selective electronic transitions between a pair of sublevels in both bands under the selection rules determined by the symmetry of the conduction and valence bands at their extremes. This phenomenon was observed in germanium at room and liquid helium temperature, by several groups of semiconductor research and was named the interband magneto-optical effect.[3],[4] Furthermore, the presence of the spin-oribt interaction would in principle give rise to the fine structures on the oscillatory behavior of the magneto-absorption. This fine structure will be observed more clearly in the rotatory dispersion rather than in the magneto-absorption since the former is influenced mainly by the difference between the dispersion of the circularly polarized wave of the right sense and that of the left one, whereas the latter phenomenon is the resultant of the absorption due to both waves. The oscillatory interband Faraday rotation was observed at first in germanium at room temperature in the steady fields up to 88 kgauss.[5] As the line shape study became one of the major problems in the analysis[6], this experiment was extended

(2) See for example; L.D. Landau and E.M. Lifshitz, *Quantum Mechanics (Non-relativistic Theory)* Ist ed. Addison-Wesley Pub. Co., Inc. Mass. (1958) p. 471.

(3) E. Burstein and G.S. Picus, Phys. Rev., **105** (1957), 1123; S. Zwerdling and B. Lax, Phys. Rev., **106** (1957), 51.

(4) E. Burstein, G.S. Picus, R.F. Wallis and F.J. Blatt, Phys. Rev., **113** (1959), 15; S. Zwerdling, B. Lax, L.M. Roth and K.J. Button, Phys. Rev., **114** (1959), 80.

(5) Y. Nishina, J. Kolodziejczak and B. Lax, Phys. Rev. Letters, **9** (1962), 55.

(6) D.L. Mitchell and R.F. Wallis, Phys. Rev., **131** (1963), 1965.

further to the low temperature region. It can be shown that the oscillatory line shape reveals the effect of the Coulomb interaction as a consequence of the exciton formation.

Another example of the interband magneto-optical effect was observed in GaSe in which the magneto-absorption and the Faraday rotation were measured simultaneously near its fundamental absorption edge.[7] Since the reduced effective mass of the electron and the hole was relatively heavy, the pulsed magnetic field up to 201 kgauss was used in this experiment to resolve magnetic structures in the spectrum.

(2) Intraband effects

In principle the experimental results on the interband effect give the band parameters which are the combination of the corresponding quantities in the conduction and the valence band. For example, interband magneto-absorption gives the reduced effective mass of the electron in the conduction band and the hole in the valence band. Similarly, the effective g-factor evaluated from the line shape of the interband Faraday effect is the sum of the effective g-factor of the electron and that of the hole. It is for this reason that the measurement on the intraband effect is necessary for obtaining the parameters of each band alone. The absorption and the rotatory dispersion of the carrier within a band can be treated classically as shown in the next section. The infrared measurements on PbTe and PbSe by Kurita et al.[8] determined the effective mass of the electron in PbTe and that of the hole in PbSe at room temperature.

Another intraband effect of our interest is the magneto-plasma effect where the reflection minimum near the plasma frequency is split into two minima which are separated by the cyclotron frequency. This work was originally performed by Lax and Wright[9] on n-type InSb with the external field perpendicular to the direction of incidence of the infrared radiation (Voigt configuration). Here this measurement was repeated with the magnetic field in the longitudinal direction, i.e. in the Faraday configuration, both at room and liquid nitrogen temperature.

(3) Lattice vibrations

In many of the semiconducting compounds the lattice vibration frequencies fall in the far-infrared wavelength region. The lattice vibration frequency of HgTe was observed by Yamamoto et al.[10] in its powdered sample. Additional transmission anomalies, presumably due to plasma resonance were observed both at 320°K and

(7) Y. Nishina, S. Kurita and S. Sugano, J. Phys. Soc. Japan, **21** (1966), 1609.

(8) S. Kurita, I. Nagasawa, K. Tanaka, Y. Nishina and T. Fukuroi, Sci. Rep. RITU, **A17** (1965), 37.

(9) B. Lax and G.B. Wright, Phys. Rev. Letters, **4** (1960), 16; See also B. Lax, "Proc. of International School of Physics, Course XXII" ed. by R.A. Smith (Academic Press, 1963), p. 274.

(10) M. Yamamoto, Bull. Phys. Soc. Japan, Okayama, Oct. 1965, vol. 3, p. 82 (in Japanese). This work was also reported at the seminar on infrared spectroscopy under the U.S.-Japan Scientific Cooperative Program at Columbus, Ohio, Sept. 1965.

at 190°K.

GaSe has a rhombohedral crystal structure which consists of the Se-Ga-Ga-Se layer as a unit.[11] Here the dominant lattice vibration is simplified to a single optical mode where these layers vibrate in the plane of the layer which is perpendicular to the c-axis.

2. Theory of magneto-optical effects

The theory of the magneto-optical absorption in semiconductors has been discussed by many investigators[1],[12],[13] in order that the observed absorption peaks could be identified in terms of the various parameters of the electronic bands. Here the phenomenological theory of the rotatory dispersion is described with particular attention to the line shape for a semiconductor with an ideal model of band structure.

2,1) Interband Faraday effect

Suppose the incoming radiation of frequency, ω, would excite an electron from a state k to another state k′ with the characteristic frequency, $\omega_{kk'}$. According to the Kramers-Heisenberg's dispersion relationship,[14] the excitation will contribute to the nondiagonal conductivity tensor element in Eq. (1) by the following equation:

$$\sigma_{ij} = -\frac{i e^2}{m^2 \hbar \omega} \sum_{kk'} \left\{ \frac{P^i_{kk'} P^j_{k'k}}{\omega_{kk'} + \omega} - \frac{P^j_{kk'} P^i_{k'k}}{\omega_{kk'} - \omega} \right\}, \tag{5}$$

where $P^i_{kk'}$ is the matrix element of the i-th component of the momentum operator,

$$\vec{P} = \vec{p} + \frac{e\vec{A}}{c} + \frac{1}{2mc^2} (\vec{S} \times \vec{\nabla} V), \tag{6}$$

which takes the spin-orbit coupling into account by the last term. We define the characteristic frequency $\omega_{kk'}{}^{\pm} = \omega_{kk'} \pm \gamma H_0$, when the external field H_0 is applied in the z-direction. Here γH_0 corresponds to the splitting due to the spin-orbit interaction and,

$$\gamma = \frac{\mu_B}{2\hbar} (g_k + g_{k'}), \tag{7}$$

where μ_B is the Bohr magneton and $g_{k(k')}$ is the effective g-factor of the electron in the $k(k')$ state. Under the weak field approximation, the terms with their singularities in Eq. (5) reduce to

(11) Z.S. Basinski, D.B. Dove and E. Mooser, Helv. Phys. Acta, **34** (1961), 373; G. Fischer, Helv. Phys. Acta, **36** (1963), 317.

(12) E. Burstein, G.S. Picus, R.F. Wallis and F.J. Blatt, Phys. Rev., **113** (1959), 15; L.M. Roth, B. Lax and S. Zwerdling, Phys. Rev., **114** (1959), 90.

(13) S. Zwerdling, W.H. Kleiner and J.P. Theriault, J. Appl. Phys. Suppl., **32** (1961), 2118.

(14) See for example; W. Heitler, *The Quantum Theory of Radiation*, 3rd Ed. (Oxford Univ. Press, London 1954) p. 190.

$$\theta \fallingdotseq \frac{-e^2}{4m^2 c \hbar n} \sum_{kk'} \frac{|P_{kk'}|^2}{\omega^2_{kk'}} \left\{ \frac{1}{(\omega^+_{kk'})^2 - \omega^2} - \frac{1}{(\omega^-_{kk'})^2 - \omega^2} \right\}, \qquad (8)$$

where n is the index of refraction. Eq. (8) is the expression for an ideal case where the relaxation time, τ, is assumed to be infinite. If the finite values of τ is introduced in Eq. (8) with the substitution of ω by $\omega - i/\tau$, the real part of this expression will give the line shape of the Faraday rotation as a function of the incident photon frequency. The line shape study is quite important for verifying the existence of the Coulomb effect between the excited electron and the hole which are produced by the energy of the incident photon.

In the absence of the Coulomb interaction the electronic transition takes place between a pair of Landau levels where the energy of the motion of the electron in the z-direction is not quantized. Hence the summation sign $\sum_{kk'}$ in Eq. (8) involves the integration over the possible values of p_z in Eq. (6). Then, in the case of the direct allowed transition Eq. (8) becomes,*

$$\theta \fallingdotseq A \sum_n \frac{\omega_c |P_{kk'}|^2}{\omega} \left\{ \frac{1}{(\omega_n - \omega - \gamma H_0)^{1/2}} - \frac{1}{(\omega_n - \omega + \gamma H_0)^{1/2}} \right\}, \qquad (9)$$

where A is a constant including the dielectric constant of the solid, $\omega_n = \omega_g + (n + 1/2)\omega_c$ and ω_c is the cyclotron frequency for the reduced mass of the electron and the hole.

If, on the other hand, the Coulomb interaction cannot be neglected, the relative motion of the electron and the hole in the direction of the external field becomes quantized. Hence $\omega_{kk'}$ is the frequency corresponding to a given state of the exciton, and the summation over p_z becomes unnecessary in Eq. (8).

If the relaxation time, τ, is introduced in Eqs. (8) and (9), the line shape of the Faraday rotation for $\gamma H_0 \tau = 1$ takes their frequency dependences as shown in Fig. 1. It can be recognized readily that the line shape for the exciton transition is symmetrical with respect to the characteristic frequency, $\omega_0 = \omega_{kk'}$ where as that for the Landau level transition is not with respect to $\omega_0 = \omega_n$. Another important characteristic in the line shape is that the sign of the rotatory peak is determined by the sign of the g-factor, or, to be more specific, by that of $g_k + g_{k'} = g_e + g_h$ in Eq. (7), where g_e and g_h are the g-factors of electron and hole, respectively.

2,2) Intraband magneto-optical effects

The magneto-optical effects due to a mobile carrier with its effective mass m^* of an isotropic band can be explained in terms of the classical equation of motion,

$$m^* \frac{\partial \vec{v}}{\partial t} + \frac{m^* \vec{v}}{\tau} = e \left[\vec{E} + \frac{1}{c} \vec{v} \times \vec{H}_0 \right]. \qquad (10)$$

*) In the derivation of Eq. (9) from Eq. (8) the terms with no singularity at $\omega_n \pm \gamma H_0$ were neglected since the photon frequency is in the neighborhood of ω_n and $\omega \gg \gamma H_0$.

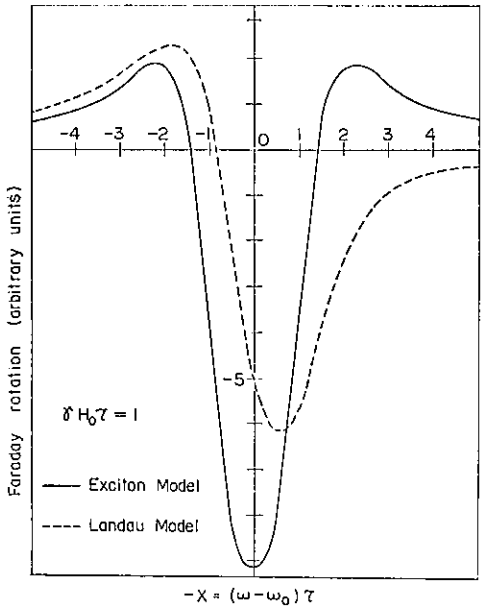

Fig. 1. Theoretical curves of the photon energy dependence of the Faraday rotation associated with the interband transition between a pair of states only with Kramers' degeneracy. A particular case of $\gamma H_0 \tau = 1$ is taken for a measure of the magnetic field.

According to the Maxwell's equations, the propagation vector, $\vec{\Gamma}$, of the plane wave with the field $\vec{E}=\vec{E}(0)\exp(i\omega t - \Gamma z)$ is related to the conductivity tensor in Eq. (1) by†

$$\Gamma_{\pm}^{2} = i\frac{4\pi\omega}{c^2}(\sigma_{xx} \mp i\sigma_{xy}) - \frac{\omega^2}{c^2}\varepsilon, \tag{11}$$

where ε is the dielectric constant of the isotropic medium.
From the definition of the conductivity tensor:

$$\vec{J} = \overleftrightarrow{\sigma}\cdot\vec{E} = Ne\vec{v}, \tag{12}$$

one can obtain the expression for the elements for the incident wave of frequency ω:

$$\sigma_{xx} = \sigma_{yy} = \frac{Ne^2}{m^*}\left\{\frac{\frac{1}{\tau} + i\omega}{\left(\frac{1}{\tau} + i\omega\right)^2 + \omega_c^2}\right\}, \tag{13,a}$$

$$\sigma_{xy} = -\sigma_{yx} = \frac{Ne^2}{m^*}\left\{\frac{\omega_c}{\left(\frac{1}{\tau} + i\omega\right)^2 + \omega_c^2}\right\}, \tag{13,b}$$

$$\sigma_{zz} = \frac{Ne^2}{m^*}\frac{1}{\frac{1}{\tau} + i\omega}, \tag{13,c}$$

†) Gaussian unit was used.

where N is the density of the carrier, $\omega_c = eH_0/m^*c$, and the external field H_0 is applied in the z-direction. τ is the relaxation time of the carrier.

The propagation constant $\Gamma_\pm$ may be expressed in terms of the complex index of refraction, $n - ik$ by

$$\Gamma_\pm \equiv \alpha_\pm + i\beta_\pm \equiv \frac{i\omega}{c}(n_\pm - ik_\pm). \tag{14}$$

For a weak magnetic field, i.e. $\sigma_{xy} \ll \sigma_{xx}$ or $\omega_c\tau \ll 1$, the approximation may hold so that $n_+ + n_- \simeq 2n$. Then the absorption coefficient α is

$$\alpha = \frac{\omega k}{c} = \frac{2\pi}{n\omega} Re(\sigma_{xx})$$

$$= \frac{2\pi Ne^2}{nm^*c} Re\left\{\frac{\frac{1}{\tau} + i\omega}{\left(\frac{1}{\tau} + i\omega\right)^2 + \omega_c^2}\right\} \tag{15}$$

$$\simeq \frac{Ne^3\lambda^2}{2\pi n c^3 \mu^* m^{*2}}, \quad \text{for} \quad \omega\tau \gg 1, \tag{16}$$

where $\mu^* = e\tau/m^*$ is the mobility of the carrier.

The expression for the Faraday effect becomes

$$\theta = \frac{2\pi}{nc} Re(\sigma_{xy}) = \frac{2\pi}{nc}\frac{Ne^2}{m^*} Re\left\{\frac{\omega_c}{\left(\frac{1}{\tau} + i\omega\right)^2 + \omega_c^2}\right\} \tag{17}$$

$$\simeq -\frac{2\pi Ne^3 H_0}{nc^2 m^{*2}\omega^2} \quad \left(\text{for} \quad \omega \gg \omega_c \quad \text{and} \quad \frac{1}{\tau}\right). \tag{18}$$

According to Eqs. (15) and (18), α and θ are proportional to $N\lambda^2/nm^{*2}$. α in Eq. (16), however, depends on the relaxation time involved in μ^*. The quantum mechanical analysis by Visuanathan[15] and by Meyer[16] shows that α is proportional to λ^3 for the scattering by ionized impurities, and to $\lambda^{2.5}$ for that by the optical mode in the lattice vibration. Because of the difference in the λ-dependence of α on the scattering mechanism, some quantitative ambiguity tends to be involved in determining the effective mass from the measurements of α. The Faraday effect, on the other hand, is rather free from the scattering mechanism. For this reason, the effective masses of free carriers in PbTe and PbSe were determined from the measurements of the Faraday rotation in the present investigation. If the energy surface is anisotropic, m^* in Eq. (18) needs some modification to account for the angular dependence of the mass values. Lax and Roth[17] calculated the particular case of germanium with four ellipsoidal energy

(15) S. Visuanathan, Phys. Rev., **120** (1960), 379; also **120** (1960), 376.
(16) H.J.G. Meyer, Phys. Rev., **112** (1958), 298.
(17) B. Lax and L.M. Roth, Phys. Rev., **98** (1955), 548.

surfaces in the ⟨111⟩ direction and the magnetic field in the ⟨100⟩ direction or the case of silicon with six ellipsoidal surfaces in the ⟨100⟩ and the magnetic field in the ⟨111⟩ direction. Then

$$\theta = \frac{Ne^2 (K+2)\, b}{2\omega c m_t n [3K - b^2 (K+1)]}, \tag{19}$$

where $K=m_l/m_t$, $b=\omega_t/\omega$ and $\omega_t=eH_0/m_t c$. With the external field in the ⟨100⟩ direction, Eq. (19) applies also in the case of PbTe and PbSe in which the prolate-ellipsoidal energy surfaces are located at the zone boundaries in the ⟨111⟩ direction. As it will be explained in Sec. 3, 3), our experimental results on the Faraday effect in n-type PbTe and p-type PbSe were found to be consistent with the theoretical interpretations in terms of this model.

2,3) Magneto-plasma effects

Another optical phenomenon of our interest on the behavior of the free carrier is the magneto-plasma effect which has been observed at room temperature in n-type InSb, InAs, HgSe[18] and n-type HgTe.[19] The phenomena of the plasma resonance may be observed rather easily by the fact that the medium becomes totally reflective for the frequency lower than the plasma frequency, ω_p, where $\omega_p{}^2=4\pi Ne^2/m^*\varepsilon_\infty$, and ε_∞ is the dielectric constant in the high frequency limit. The reason may be recognized readily as follows. The reflectivity, R, of the light normally incident on the medium is given by,

$$R = \frac{(n-1)^2 + k^2}{(n+1)^2 + k^2}. \tag{20}$$

For a dispersive medium like in our case ($\omega\tau \gg 1$), it may be approximated by,

$$R = \frac{(n-1)^2}{(n+1)^2}. \tag{21}$$

For a longitudinal propagation, i.e. $\vec{\Gamma} // \vec{H}_0$ the waves in the medium can be described in terms of two circularly polarized waves of different senses with the corresponding values of the indices of refraction, given by the following expression:

$$n_\pm{}^2 = \varepsilon_\infty \left[1 - \frac{\omega_p{}^2}{\omega(\omega \pm \omega_c)}\right]. \tag{22}$$

Here the contributions from the lattice vibrations are neglected. For each circularly polarized wave, therefore, the index of refraction becomes zero at the frequency,

$$\omega_\pm = \frac{1}{2}\left[\{\omega_c{}^2 + 4\omega_p{}^2\}^{1/2} \pm \omega_c\right], \tag{23}$$

corresponding to $n_\pm=0$.

(18) G.B. Wright and B. Lax, J. Appl. Phys. Suppl., **32** (1961), 2113.
(19) L. Sniadower, V.I. Ivanov-Omsky and Z. Dziuba, Phys. Stat. Solidi (Germany), **8** (1965), K43.

For the frequency $\omega<\omega_{\pm}$, $(n_{\pm}-ik_{\pm})$ becomes pure imaginary, and this implies total reflection, where $R=1$. It may be recognized from Eq. (22), that, for two frequencies $\omega_{m\pm}$ slightly greater than $\omega_{\pm}$, $n_{\pm}$ becomes unity, where the reflectivity in Eq. (20) gives two minima, and from Eq. (22),

$$\omega_{m\pm}=\omega_p\left(1+\frac{1}{2\,\varepsilon_\infty}\right)\pm\frac{\omega_c}{2}+\frac{1}{8}\frac{\omega_c^2}{\omega_p}\left(1-\frac{1}{2\,\varepsilon_\infty}\right). \tag{24}$$

In the absence of the magnetic field, these two minima coincides, but for a magnetic field sufficiently large, one can observe two minima separated by the cyclotron frequency ω_c. This splitting in the reflectivity minima gives the direct measure of the effective mass m^*.

3. Experimental results

3,1) Interband magneto-optical effects in germanium

The interband magneto-optical effects in germanium has been a subject of experimental and theoretical interests for almost a decade.[20] Recently more attention has been focussed on the Faraday[21] and the Voigt[22] effect associated with

(20) For an early review of this subject see for example B. Lax and S. Zwerdling, *Progress in Semiconductors*, ed. by. A.F. Gibson et al. Heywood & Co., London (1960), vol. 5, p. 221.

(21) For theoretical analysis;
M.J. Stephen and A.D. Lidiard, J. Phys. Chem. Solids, **9** (1958), 43.
H.S. Bennett and E.A. Stern, Univ. of Maryland Technical Rep. No. 197, (1960) (unpublished).
B. Lax, Proc. of the International Conference on Semiconductor Physics, Prague, 1960 (Czechoslovakian Academy of Sciences, Prague, 1961) p. 321.
B. Lax and Y. Nishina, Phys. Rev. Letters, **6** (1961), 464.
B. Lax and Y. Nishina, J. Appl. Phys. Suppl., **32** (1961), 2128.
M. Suffczynski, Proc. Phys. Soc. (London), **77** (1961), 1042.
I.M. Boswarva, R.E. Howard and A.D. Lidiard, Proc. Roy. Soc. (London), **A269** (1962), 125.
J. Kołodziejczak, B. Lax and Y. Nishina, Phys. Rev., **128** (1962), 2655.
J. Halpern, B. Lax and Y. Nishina, Phys. Rev., **134** (1964), A140.
I.M. Boswarva and A.D. Lidiard, Proc. Roy., Soc. (London) **278** (1964) 588.
L.M. Roth. Phys. Rev., **133** (1964), A542.
H.S. Bennett and E.A. Stern, Phys. Rev., **137** (1965), A448.
T. Murao and A. Ebina, J. Phys. Soc. Japan, **20** (1965), 997.

For experimental results:
S.D. Smith, T.S. Moss and K.W. Taylor, J. Phys. Chem. Solids, **11** (1959), 131.
R.N. Brown and B. Lax, Bull. Amer. Phys. Soc. Ser. II, **4** (1959), 133; See also B. Lax, *Prog. of Semiconductors*, ed. by A.F. Gibson et al. Heywood & Co., London (1960), Vol 5, p. 254.
A.K. Walton and T.S. Moss, J. Appl. Phys., **30** (1959), 951.
B. Hartmann and B. Kleman, Arkiv Fysik, **18** (1960), 75.
M. Cardona, Phys. Rev., **121** (1961), 752.
A.K. Walton and T.S. Moss, Proc. Phys. Soc. (London), **78** (1961), 1393.
Y. Nishina, J. Kołodziejczak and B. Lax, Phys. Rev. Letters, **9** (1962), 55.
H. Piller and R.F. Potter, Phys. Rev. Letters, **9** (1962), 203.

the interband transitions. One of the main problems which required careful analysis was the effect of the Coulomb interaction between the electron and the hole on the rotatory dispersion. Although the use of a high magnetic field in the measurement of the interband Faraday effect exhibited the existence of the fine structures at room temperature, the line width for each singularity was found to be too broad for clearly discriminating one from the other. Consequently the previous experiment on germanium was extended to the temperature region near 10°K[23]. The grating spectrometer of Perkin-Elmer Model 99G[24] was used for this measurement. The rotation of the plane of polarization was measured with the optical bridge described previously.[5],[25] A Bitter solenoid of Helmholtz-type produced the maximum field of 59 kgauss for the direct current of 10,000 amp. Since this magnet could be rotated by 90° around the transverse horizontal axis, it was possible to measure both Faraday and Voigt effect with the optical arrangement common to both configuration of the field. With this optical arrangement it was more convenient for us to measure the rotation rather than phase shift in the Voigt effect. The rotation angle ϕ may be approximated in the weak field region by the real part of $\frac{2\pi}{nc}(\sigma_{xx}-\sigma_{zz})$ in Eq. (4).

Since the thin sample (about 4μ thick) was glued to a glass substrate for its mechanical reinforcement, the difference in the thermal expansion coefficient of glass and that of the sample gave rise to the strain in its transverse plane. This

E.D. Palik, S. Teitler, B. Henvis and R.F. Wallis, "Proc. of the International Conf. on the Phys. of Semiconductors, Exeter, 1962" (The Institute of Physics and the Physical Society, London, 1962), p. 288.
T.S. Moss, A.K. Walton, and B. Ellis, "Proc. of the International Conf. on the Phys. of Semiconductors, Exeter, 1962" (The Institute of Physics and the Physical Society, London, 1962), p. 295.
S.D. Smith, C.R. Pidgeon and V. Prosser, "Proc. of the International Conf. on the Physics of Semiconductors, Exeter, 1962" (The Institute of Physics and the Physical Society, London, 1962) p. 301.
H. Piller and V.A. Patton, Phys. Rev., **129** (1963), 1169.
D.L. Mitchell and R.F. Wallis, Phys. Rev., **131** (1963), 1965.
A. Ebina, T. Koda and S. Shionoya, J. Phys. Chem. Solids, **26** (1965), 1497.
M. Balkanski, E. Amzallag and D. Langer, J. Phys. Chem. Solids, **27** (1966), 299.
C.R. Pidgeon, C.J. Summers, T. Arai and S.D. Smith, "Proc. of the International Conf. on Physics of Semiconductors, Paris, 1964", (Dunod, Paris, 1964), p. 289.
H. Piller, "Proc. of the International Conf. on Physics of Semiconductors, Paris, 1964" (Dunod, Paris, 1964), p. 297.
J.L. Callies and C. Rigaux, "Proc. of the International Conf. on Physics of Semiconductors, Paris, 1964", (Dunod, Paris 1964), p. 305.
Y. Nishina, J. Kołodziejczak and B. Lax, "Proc. of the International Conf. on Physics of Semiconductors, Paris, 1964", (Dunod, Paris, 1964), p. 867.

(22) B. Lax, Y. Nishina and J. Kołodziejczak, Bull. Amer. Phys. Soc. Ser. II, **7** (1962), 535.
Y. Nishina, J. Kołodziejczak and B. Lax, ibid.
M. Cardona, Helv. Phys. Acta, **34** (1961), 796.

(23) This experiment was carried out at National Magnet Laboratory, M.I.T. at Cambridge, Mass., U.S.A. by one of the authors (YN).

(24) Made by the Perkin-Elmer Corp,. Norwalk, Connecticut, U.S.A.

(25) Y. Nishina, Bussei, **5** (1964), 354 (in Japanese).

deformation removed the degeneracy at Γ-point of the valence band. Then the absorption peak for the ground state of the exciton near the absorption edge was split into two peaks with the separation of 4.5 meV in the absence of the external field. This removal of degeneracy enabled us to single out the rotatory dispersion associated with the interband transition between a pair of non-degenerate energy levels. The experimental results on the Faraday and the Voigt effect at 39.5 kgauss are shown in Figs. 2 and 3. As it was explained in the Section 2, the line shape could be used to verify the existence of the exciton effect. The expressions for the Faraday angle for the Landau level transitions, θ_n, and for the exciton transition, θ_k are given as follows:

$$\theta_n = \frac{\omega_c}{4\pi\sqrt{\tau_n}}\left(\frac{\mu}{\hbar}\right)^{3/2} A\left[\left\{\frac{\sqrt{(X_n+Y_n)^2+1}+X_n+Y_n}{(X_n+Y_n)^2+1}\right\}^{1/2} - \left\{\frac{\sqrt{(X_n-Y_n)^2+1}+X_n-Y_n}{(X_n-Y_n)^2+1}\right\}^{1/2}\right], \tag{25}$$

and

$$\theta_k = A\left\{\frac{X_k+Y_k}{(X_k+Y_k)^2+1} - \frac{X_k-Y_k}{(X_k-Y_k)^2+1}\right\}, \tag{26}$$

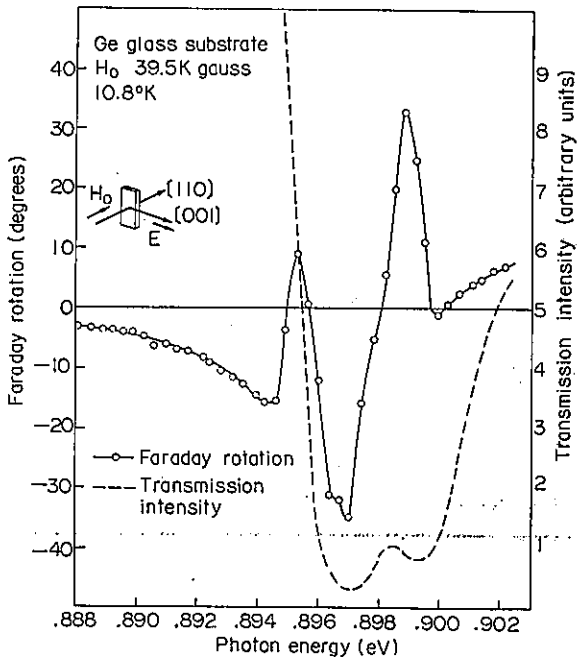

Fig. 2. Experimental results of the Faraday rotation in Ge at 10.8°K with the magnetic field of 39.5 kgauss. Glass substrate gave rise to the removal of degeneracy at Γ-point in the valence band.

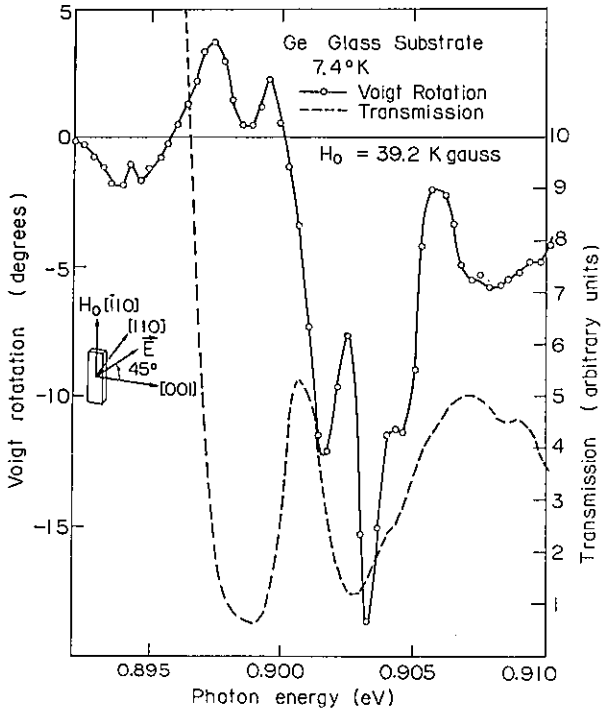

Fig. 3. Experimental results of the Voigt effect in Ge at 7.4°K with the magnetic field of 39.2 kgauss.

where $X_{n,k}=(\omega_{n,k}-\omega)\tau_{n,k}$, $Y_{n,k}=\gamma_{n,k}H_0\tau_{n,k}$ and A is a constant given by the product of the momentum matrix element and a factor consisting of universal constants. ω_c is the cyclotron frequency for the effective reduced mass, μ, of the electron and the hole and τ the relaxation time for the transition. If the tails of the Faraday singularities at higher photon energies were subtracted, the two positive peaks in Fig. 2 could be fitted with the curve for θ_k given by Eq. (26). The parameters used for these calculations are given in Table 1 and the comparison with the calculations are shown in Fig. 4. The calculated curve from Eq. (25), however, with the negligence of the Coulomb interaction does not fit the experimental points. The

Table 1. The parameters used for the theoretical fit of the Faraday rotation for H_0=39.5 kgauss in Fig. 2. With the subtraction of the background rotation.

Peak in Fig. 4	a	b
g-factor	−1.2	−1.4
τ_k(sec)	7.9×10^{-13}	5.7×10^{-13}
Y_k	−0.15	−0.14

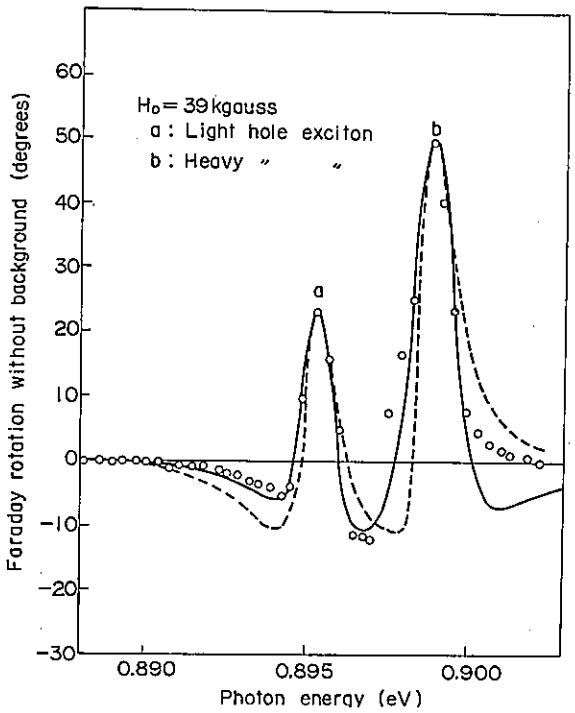

Fig. 4. Theoretical fit of the Faraday rotation for H_0=39.5 kgauss. The solid line is θ_k of Eq. (26) with the parameters given in Table 1. The dotted line is the Faraday rotation for a transition between a pair of Landau levels as given by θ_n in Eq. (25) with the same value of Y_n as Y_k.

discrepancy seems to indicate that the Coulomb interaction cannot be neglected in the determination of electronic energy levels.

Furthermore, the presence of the strain caused the mixing of the states with different values of magnetic quantum number, M_J. Since the degree of such mixing changed as a function of the external field, the sign of the Faraday rotation reversed when the magnetic field in the ⟨110⟩ direction was increased beyond about 45 kgauss. This phenomenon may be recognized if Fig. 2 is compared with Fig. 5, where the negative peak at 0.8985 eV with H_0=56.7 kgauss corresponds to the positive one at 0.8955 eV with H_0=39.5 kgauss. According to the theoretical analysis by Suzuki et al.,[26] this reversal is caused by the mixing of the wave function for M_J=3/2, n=0 with that for M_J=−1/2, n=0 and 2 in the valence band as a combined effect of the external field and the strain induced in the sample. Fig. 5 shows also an example that the electronic fine structures could be discriminated more easily with the measurement of the Faraday rotation rather than the magneto-absorption for a given resolution of the spectrometer system. Because the two oscillatory Faraday peaks at 0.8985 eV and at 0.9010 eV in Fig. 5

(26) K. Suzuki, E. Hanamura, M. Okazaki and H. Hasegawa, to be published; K. Suzuki, Doctoral Thesis, Dept. of Physics, Univ. of Tokyo, (1965).

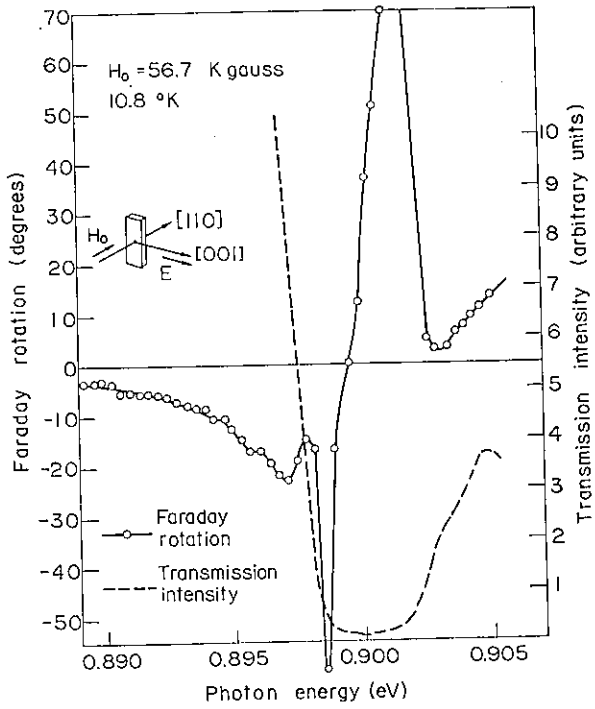

Fig. 5. The Faraday rotation of Ge at 10.8°K for H_0=56.7 kgauss.

cannot be associated with two distinctive peaks in the transmission, but merely with one broad band of absorption.

3,2) Interband magneto-optical effects in GaSe

Magneto-optical measurements in germanium[21),(27),(28)] have revealed that the Coulomb interaction between the electron in the conduction band and the hole in the valence band is a dominant factor to cause the optical properties which are not expected of the electronic transitions between a pair of Landau levels. As for the theoretical analysis this experimental results may be analysed with a hydrogen-like model where the positive ion is replaced by a hole, and the vacuum space between the hole and the electron is filled with a dielectric medium. The theoretical analysis for the electronic structures in the external magnetic field was given by Elliott and Loudon[29)] and also by Hasegawa and Howard.[30)] The problem can be solved either for the strong or weak field limit. The most difficult case lies in the intermediate range where the Coulomb energy is comparable to the cyclotron energy of an electron-hole pair. The theoretical problem may be simplified considerably if the motions of electrons and holes are restricted in a

(27) S. Zwerdling, B. Lax, L.M. Roth and K.J. Button, Phys. Rev., **114** (1959), 80.
(28) D.F. Edwards and V.J. Lazazzera, Phys. Rev., **120** (1960), 420.
(29) R.J. Elliott and R. Loudon, J. Phys. Chem. Solids, **15** (1960), 196.
(30) H. Hasegawa and R.E. Howard, J. Phys. Chem. Solids, **21** (1961), 179.

plane. This condition may serve as a rough approximation in the case of GaSe which is one of the semiconducting substances with layer structure and the electronic interactions between neighboring layers are small compared with those in a layer.[11] The interband magneto-absorption and the Faraday rotation were measured with the use of a superconducting solenoid.[31] This magnet had a nearly elliptical bore so that the light flux out of a monochromator slit could be transmitted through the bore without receiving too much disturbance from its geometry., The calibration of the field was given in terms of the magneto-resistance in an Sb-probe. The measurements of the interband Faraday effect in GaSe at 1.77°K up to the field of 17 kgauss did not quite resolve the fine structures associated with the exciton lines in the magnetic field. The energy gap between both extremes of the conduction and of the valence band was found in the vicinity of 2 eV. Since the detector (photomultiplier tube) in this photon energy range had a fast response, the magneto-optical measurement was continued with the use of a pulsed magnet[32] which could produce the maximum field of 201 kgauss through the electrical discharge of a 3000μF condenser bank.[7] The sample was sandwiched between a pair of polaroid sheet with their polarizing angle at 45 degrees with respect to each other. It was placed in the center of the magnet bore and was immersed in the liquid nitrogen. Then the radiation out of the analyser was passed through a monochromator and was detected with a S-20 type photomultiplier. The change in the output during a single sweep of a pulse field was displayed on an oscilloscope and was photographed by a Type-47 polaroid film. The measurement of the detector output for both polarities of the magnetic field gave simultaneously the Faraday rotation angle and the magneto-absorption.[33] Fig. 6 shows a typical example of the measurements in the external fields of 140 and 201 kgauss. The three major peaks in the absorption at 201 kgauss coincide in their respective values of the photon energy with the negative peaks of the Faraday rotation for the same intensity of the magnetic field. As it was explained in the previous section, this characteristic in the line shape implies that the oscillatory behavior of the Faraday rotation and the magneto-absorption is associated with the electronic transition to an exciton level. This interpretation is also supported by our observation that the amplitude of the Faraday rotation decreases considerably as one goes from the peak with the owest photon energy to the higher ones. If the direct electronic transitions take place between the Landau levels, the oscillator strength for each transition is

(31) Y. Nishina, S. Kurita and K. Tanaka, "Proc. International Symposium on Magnet Technology", ed. by H. Brechna and H.S. Gordon, NBS., U.S. Dept. of Commerce, Springfield Va., (1965), p. 525.

(32) For an example of this type of magnet see, K. Aoyagi, A. Misu and S. Sugano, J. Phys. Soc. Japan, **18** (1963), 1448.

(33) For details of the experimental arrangement see Y. Nishina, S. Kurita and S. Sugano, to be published in the Proc. of the International Colloqium for the High Magnetic Field, Grenoble, France 1966.

independent of the magnetic quantum number, n, whereas it decreases with increasing value of n in the presence of the Coulomb interaction. For an ideal case of the two dimensional crystal the oscillator strength for the electric dipole transition to the exciton level in the absence of the external field decreases as $(n+1/2)^{-3}$, (n=0, 1, 2....). For a three dimensional crystal it is expected to decrease as n^{-3} (n=1, 2, 3,....)[34].

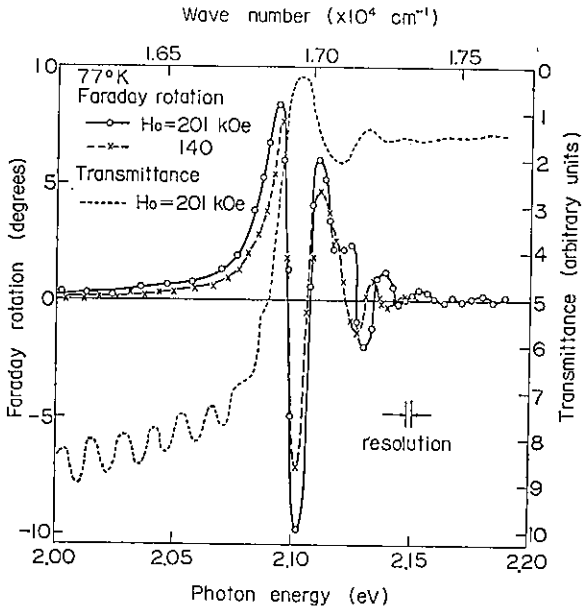

Fig. 6. The Faraday rotation in GaSe at 77°K in the fields of 140 and 201 kgauss and the magneto-absorption in the field of 201 kgauss. Sample thickness was 15.4μ.

Table 2. The electronic band parameters deduced from the Faraday rotation measurements at 77°K in comparison with those obtained from the magneto-absorption measurements by Aoyagi et al.[34] at 4.2°K.

	77°K	4.2°K[34]
Energy Gap (eV)	2.127	2.133
Reduced Effective Mass $\frac{m^*}{m_0}$	0.13	0.138
Effective g-Factor $g_{//}=g_{e//}+g_{h//}$	3.3	
Relaxation Time (sec)	1.8×10^{-13}	
Exciton Binding Energy (meV)	26	20

(34) K. Aoyagi, A. Misu, G. Kuwabara, Y. Nishina, S. Kurita, T. Fukuroi, O. Akimoto, H. Hasegawa, M. Shinada and S. Sugano, "Proc. Int. Conf. on Physics of Semiconditors, Kyoto 1966" J. Phys, Soc. Japan **21** Suppl. (1966) 174. Also Tech. Rep. ISSP. Univ. of Tokyo. Ser. A, No. 205 (1966).

The band parameters deduced from the above measurements are given in Table 2.

3,3) Free carrier absorption and the Faraday effect in PbTe and PbSe

The band structures of PbTe and PbSe have been studied in terms of their optical properties.[35],[36] The experimental results on the Shubnikov-de Haas effect of these compounds[37] indicated that the energy surfaces of electrons and holes were (111) prolate-ellipsoides at the zone boundaries. In PbTe the existence of such energy surfaces were confirmed by the cyclotron resonance experiments both in n- and p-type specimens[38],[39] at 1.8°K. Further experimental investigations by Cuff et al.[40] and the theoretical analysis by Dimmock and Wright[41] showed that the energy surfaces of electrons and holes in PbSe were quite similar to those in PbTe. In PbTe the reflectivity measurements[36],[42] at the plasma edge gave the effective susceptibility (conductivity) mass of the electrons consistent with the above model with respect to their dependence on the carrier concentration and the temperature. Similar measurements on holes in p-type samples, however, gave some evidence for the existence of another kind of hole at Γ-point besides the one for the ellipsoids.[38] The optical properties of PbSe has not been studied so well as PbTe except the interband magneto-optical measurements by Mitchell et al.[43] who determined the energy gap and the reduced effective mass of electrons and holes at low temperatures. The quantitative difference in the band parameters of these substances, however, lies in a slightly higher mass and smaller anisotropy of PbSe compared with those of PbTe. The free carrier optical measurement is still important because of the following reasons:

(1) The mass parameters obtained from free-carrier measurement are those for the carriers populating in each band only. These would complement the information obtained from the interband magneto-optical measurements, so that the reduced mass parameters of electrons and holes involved with the interband transition may be separated into each mass parameter at a given temperature and carrier density.

(2) The effective mass parameter measured by the free carrier Faraday effect is the cyclotron mass, m_c, whereas the parameters given by the reflective anomaly

(35) W.W. Scanlon, *Solid State Phys*, **9**, ed. by F. Seitz and D. Turnbull (Academic Press, N. Y., 1960), p. 83.
(36) J.R. Dixon and H.R. Riedl, Phys. Rev., **138** (1965), A 873.
(37) K.F. Cuff, M.R. Ellett and C.D. Kuglin, J. Appl. Phys. Suppl., **32** (1961), 2179.
(38) P.J. Stiles, E. Burstein and D.N. Langenberg, Phys. Rev. Letters, **9** (1962), 257.
(39) R. Nii, J. Phys. Soc. Japan, **19** (1964), 58.
(40) K.F. Cuff, M.R. Ellett, C.D. Kuglin and L.R. Williams, "Proc. of International Conf. on Phys. of Semiconductors, Paris, 1964", (Dunod, Paris, 1964), p. 677; M.R. Ellett and K.F. Cuff, Bull. Am. Phys. Soc. Ser. II, **8** (1963), 601.
(41) J.O. Dimmock and G.B. Wright, Phys. Rev., **135** (1864), A821.
(42) H.A. Lyden, Phys. Rev., **135** (1964), A514.
(43) D.L. Mitchell, E.D. Palik and J.N. Zemel, "Proc. International Conf. on Phys. of Semiconductors, Paris, 1964", (Dunod, Paris, 1964), p. 325.

near the plasma resonance frequency is the susceptibility mass, m_s. Although m_c is equal to m_s for the carrier with a spherical constant-energy surface, they are different in general in the case of a non-spherical energy surface. The energy surfaces of the carriers in PbTe and PbSe are characterized by the ⟨111⟩ prolate ellipsoids of revolution. If the external magnetic field is applied in the ⟨100⟩ direction as in the present case of experiment, m_c, obtained from the Faraday effect is given by,[17]

$$m_c = m_{F(100)} = \sqrt{\frac{3\,m_t^2\,m_l}{2\,m_t + m_l}}\,, \tag{27}$$

where m_t and m_l are the transverse and longitudinal masses of the ellipsoid, respectively.

On the other hand, the m_s obtained from the plasma reflection is given by,[36),(42)]

$$m_s = m_p = \frac{3\,m_t\,m_l}{2\,m_l + m_t}\,. \tag{28}$$

These two types of optical measurement, therefore, would determine the parameters of the ellipsoidal energy surfaces. In principle such determination of the mass parameters could be given also by a cyclotron resonance experiment. But the optical measurements mentioned above have the advantage that they may be carried out over the wider range of temperature and carrier concentration, mainly because the electromagnetic wave used for an optical experiment lies in much higher frequency region than that for the cyclotron resonance, thus the optical measurements may be free from the effect of the relaxation effect of the carriers.

Table 3. Electrical properties of PbTe and PbSe samples.

Sample and type	295°K			77°K			4.2°K		
	N	ρ	μ_H	N	ρ	μ_H	N	ρ	μ_H
p-PbTe No. 1	2.04×10^{18}	3.67×10^{-2}	8.35×10^{2}	2.68×10^{18}	1.61×10^{-4}	1.45×10^{4}	2.45×10^{18}	1.09×10^{-5}	2.47×10^{5}
p-PbTe No. 2	1.68×10^{18}	4.35×10^{-3}	8.43×10^{2}	2.58×10^{18}	1.67×10^{-4}	1.46×10^{4}	2.45×10^{18}	7.75×10^{-6}	3.3×10^{5}
n-PbTe No. 1	3.58×10^{17}	1.16×10^{-2}	1.50×10^{3}	3.67×10^{17}	5.58×10^{-4}	2.74×10^{4}	3.37×10^{17}	4.18×10^{-6}	4.32×10^{6}
n-PbTe No. 2	3.10×10^{17}	1.39×10^{-2}	1.45×10^{3}	3.10×10^{17}	6.89×10^{-4}	2.64×10^{4}	3.20×10^{17}	7.94×10^{-6}	2.70×10^{6}
p-PbSe No. 1	2.67×10^{18}	3.17×10^{-3}	7.39×10^{2}	2.69×10^{18}	5.94×10^{-4}	3.91×10^{3}	2.81×10^{18}	5.47×10^{-5}	4.06×10^{4}
p-PbSe No. 2	2.35×10^{18}	2.66×10^{-3}	9.76×10^{3}	2.68×10^{18}	1.58×10^{-4}	1.48×10^{4}	2.71×10^{18}	2.23×10^{-5}	1.04×10^{5}

N; charge carrier density in cm^{-3}
ρ; resistivity in ohm-cm
μ_H; Hall mobility in cm^2/volt sec.

Kurita et al.[8] measured the free carrier absorption and the Faraday effect of both n- and p-type PbTe and p-type PbSe with the electrical properties shown in Table 3. The measurements were carried out at room temperature in the wavelength range from 3.8μ to 15μ by means of a Carl Leiss double monochromator[44] with a rock salt prism.

The direct energy gaps evaluated from the wavelength dependence of the absorption for the above samples were,

$E_g = (0.314 \pm 0.005)$ eV at 295°K p-PbTe No. 1,

$E_g = (0.271 \pm 0.005)$ eV at 295°K p-PbSe No. 1.

These energy values are in agreement with those observed by Scanlon,[45] who found them to be 0.32 eV for PbTe and 0.29 eV for PbSe, respectively. Since the samples used in our measurements were as thin as 50–180μ, no experimental evidence was observed for the indirect gap as pointed out by Scanlon.[45] Also the effective masses given by Eq. (27) were deduced from the measurements of the Faraday effect as follows:

$m_{F(100)} = (0.110 \pm 0.005)\, m_0$ for electrons (at 298°K n-PbTe Nos. 1 and 2),

$m_{F(100)} = (0.139 \pm 0.005)\, m_0$ for holes (at 294°K p-PbSe No. 1).

The value of the effective mass of the electron in PbTe is slightly higher than those observed by Walton and Moss[46] who gave $m_{F(100)}=0.083 \pm 0.004$ for the concentration of $(2.7 \sim 1.2) \times 10^{17} \mathrm{cm}^{-3}$, and also by Lyden[42] whose measured values of m_t and m_l lead to $m_{F(100)}=0.11$ for the concentration of $(2.9 \sim 3.8) \times 10^{18}\ \mathrm{cm}^{-3}$.

To our knowledge there has been no report on the optical measurement of the effective mass of holes in PbSe at room temperature. For a rough comparison the value of m_F at $1.1 \sim 4.2$°K was calculated from the measurements of the Shubnikov-de Haas effect by Cuff et al.,[40] which turned out to be $0.058\, m_0$ for the hole concentration $(2 \times 10^{18} \sim 10^{19}\ \mathrm{cm}^{-3})$.

Another kind of effective mass parameter can be obtained from the thermoelectric power measurement. It is denoted by the density-of-state mass, m_D^*, to take into account the statistical distribution of the carrier energy. If the number of the equivalent ellipsoids is η, m_D^* is given by,[42]

(44) Made by the Carl Leiss, 26 Feuerbachstr. Berlin-Steglitz, Germany.

(45) W.W. Scanlon, "Proc. International Conf. on Phys. of Semiconductors, Rochester, N.Y. (1958)", J. Phys. Chem. Solids, **8** (1958), 423. Also see p. 116 of ref. (35).

(46) A.K. Walton and T.S. Moss, Proc. Phys. Soc., **81** (1963) 509; Also see for original results A.K. Walton, T.S. Moss and B. Ellis, Proc. Phys. Soc., **79** (1962) 1065.

$$m_D^* = \eta^{2/3} m_l K^{1/3}, \tag{29}$$

where $K=m_l/m_t$ is the mass ratio for the case of isotropic scattering. The combination of Eq. (27) with Eq. (29) gives,

$$\frac{m_D^*}{m_F^*{}_{(100)}} = \eta^{2/3} K^{1/3} \left(\frac{3K}{K+2}\right)^{-1/2}. \tag{30}$$

Thus the η and K could be evaluated from our results with the use of the experimental data on the thermoelectric power for PbTe by Gershtein et al.[47] and for PbSe by Smirnov et al.[48] It was found that,

$K = 3\ (\pm 2)$ for electrons in PbTe,
$\eta = 4$

$K = 2\ (\pm 1)$ for holes in PbSe,
$\eta = 4$

both at room temperature. These experimental results indicate a high degree of similarity between the conduction band of PbTe and the valence band of PbSe, and confirm the conclusion of Cuff et al.[40]

The band structures of PbTe and PbSe are strongly dependent on the temperature and carrier concentration. The above investigation was continued with p-type PbSe at room temperature.[49] The wavelength dependence of the Faraday rotation angle is shown in Fig. 7 for several samples with their hole concentrations ranging from $4.05\times10^{17}\mathrm{cm}^{-3}$ to $6.25\times10^{18}\mathrm{cm}^{-3}$. The effective mass of the hole was found to increase from $0.09\,m_0$ to $0.11\,m_0$*) in the above range of concentration. The above result gives another example of the importance of the non-parabolicity in the determination of the band structure in lead salts. For more consistent treatment of this problem, it would be highly desirable to measure the Faraday rotation and the plasma reflection at low temperatures in various ranges of carrier concentration.

3,4) Magneto-plasma reflection in InSb

According to Eq. (23) the classical dispersion theory predicts the splitting of the anomaly near the plasma reflection edge. Its experimental verification, however, has been limited to rather small varieties of semiconductors,[9],[18],[19] since

(47) E.Z. Gershtein, T.S. Stavitskaya and L.S. Stil'bans, Zhur. Tekn. Fiz., **27** (1957), 2474; Sov. Phys.-Technical Phys., **2** (1957), 2302.
(48) I.A. Smirnov, B. Ya. Moishes and E.D. Neusberg, Fiz. Tverd. Tela, **2** (1960), 1992; Sov. Phys.-Solid State, **2** (1960), 1793.
(49) S. Kurita, Y. Nishina and T. Fukuroi, Bull. Phys. Soc. Japan, Waseda Univ., Tokyo 1965, Vol. 2, 133 (in Japanese).
*) The values of the effective masses were corrected from those in ref. (8) because of the carrier population effect in the long wavelength limit.[50] The details of the calculation are subject to future publication.[51]
(50) E.A. Stern, Phys. Rev. Letters, **15** (1965), 62.
(51) S. Kurita, to be published.

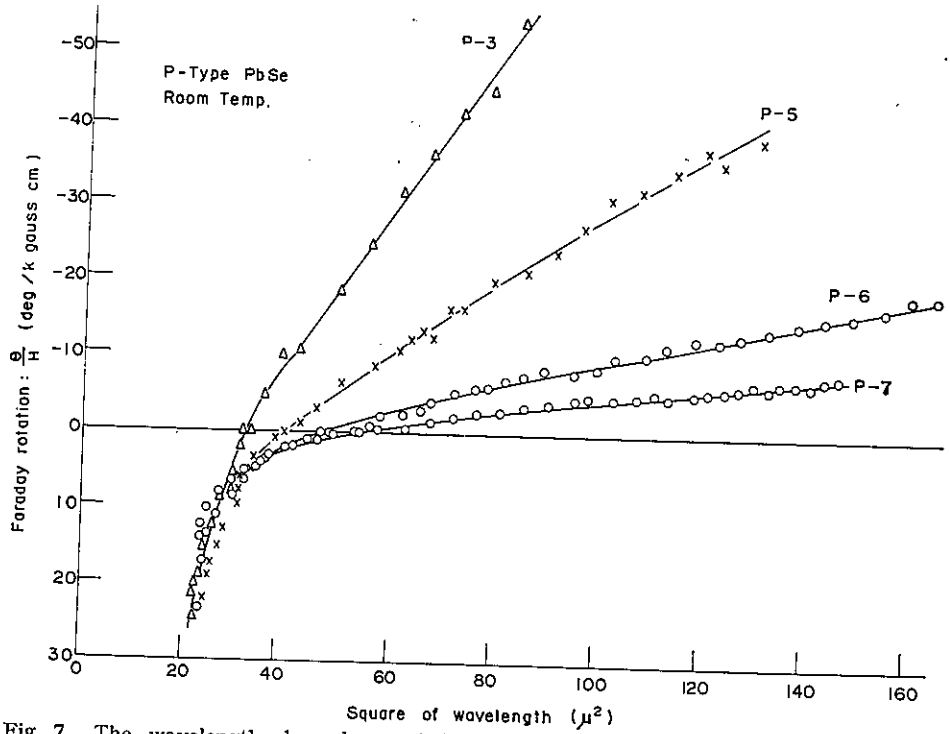

Fig. 7. The wavelength dependence of the Faraday rotation in p-type PbSe at room temperature. The hole concentrations at 77°K were
P-3: 26.9×10^{17}cm^{-3} P-5: 15.6×10^{17}cm^{-3}
P-6: 6.57×10^{17}cm^{-3} P-7: 4.05×10^{17}cm^{-3}, respectively.
The samples were degenerate at room temperature.

the splitting may be observed in practice only for the free carrier with its effective mass in the order of $0.05m_0$ or less†). In spite of this experimental difficulty, the measurement of the magneto-plasma reflection has the unique advantage over that of the zero-field plasma reflection by the following reasons:

(1) In an ordinary zero-field measurement, the effective mass may be evaluated only with the knowledge of the carrier concentration deduced from the Hall coefficient together with the value of dielectric constant obtained from the reflectivity at high frequency limit. Since the concentration of the carriers may be measured with the accuracy of 5% or so, the accuracy of the effective mass cannot be higher. On the other hand, the experiment on the magneto-plasma reflection determines the effective mass directly from the energy splitting ($\hbar\omega_c$) between the two minima in reflection coefficient in the external magnetic field. It may be recognized from Eqs. (21), (22) and (24) that in case of spherical energy surfaces the use of the reflectivity data in the absence of the field together with those for the magneto-reflection gives the simultaneous measurements of the

†) The intensity of the magnetic field used in this experiment is the order of 50 kgauss or so.

dielectric constant, carrier density and the effective mass. In addition the numerical analysis of the above data can give the relaxation time of the carriers.

(2) The measurement of the magneto-reflection under the transverse and the longitudinal configuration of the magnetic field gives the information on the anisotropy of the energy surfaces of the carrier. The explanation is quite similar to that given in Sec. 3.3.

(3) The field dependence of the magneto-reflection may give the band parameters for the non-parabolicity.

The measured effective mass value of electrons in InSb[18] was found reasonably consistent with the numerical estimation in terms of the Kane's theory.[52]

More detailed study on the band structure of InSb becomes possible if the above measurements are extended to low temperature region so that the relationship between the energy gap, the effective mass and the carrier concentration may be considered in the light of Kane's work. Jimbo et al.[53] carried out the measurement on the magneto-plasma effect of InSb both at 300°K and 90°K.

The optical arrangement consisted of the Carl Leiss double monochromator[44]

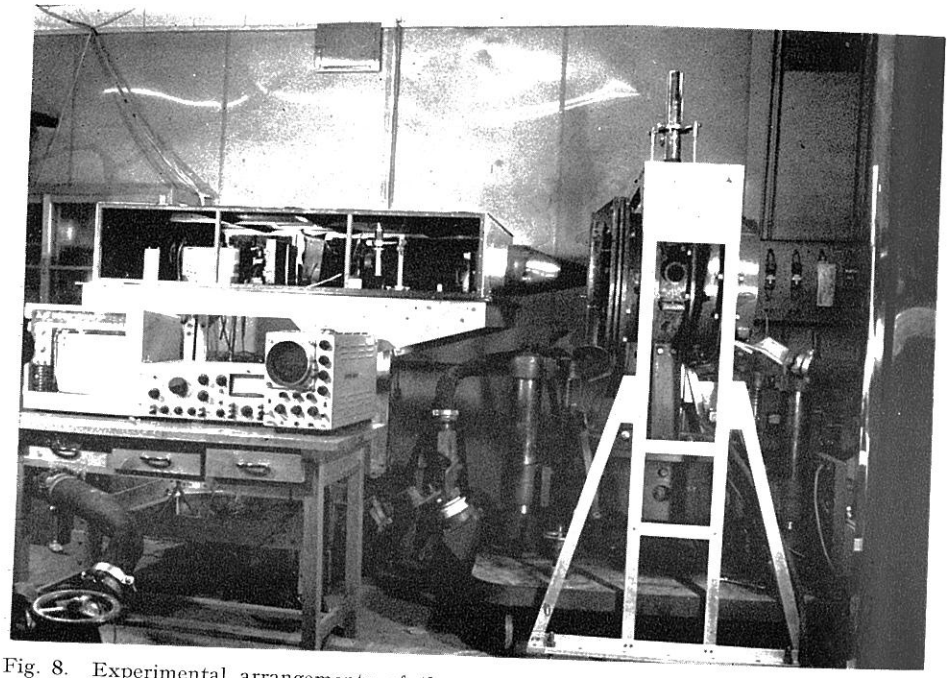

Fig. 8. Experimental arrangements of the magneto-plasma measurements. The spectrometer system is arranged on the optical table on the left. The monochromatic radiation is sent into the center of the Bitter solenoid on the right. The sample was cooled by a cold finger of a glass dewar with rock-salt windows.

(52) E.O. Kane, J. Phys. Chem. Solids, **1** (1957), 249.

(53) T. Jimbo, Y. Nishina, K. Tanaka and T. Fukuroi, Bull. Phys. Soc. Japan, Tokyo, March 1966, Vol. 4, p. 174, (in Japanese); also the Master's thesis by T. Jimbo, Phys. Dept. Tohoku Univ., 1966.

with a pair of KBr prisms which could cover the wavelength range from 11μ to 23μ. A sensitive thermocouple was used as the detector which was coupled with the preamplifier of the Perkin-Elmer Corp.[24] and the Model JB–5 lock-in amplifier.[54] A Bitter solenoid of Helmholtz Type was used to give the maximum field of 39 kgauss with the direct exciting current of 7,000 amp. The whole experimental arrangements are shown in the Fig. 8.

Two different values of the electron concentration in n-type InSb were chosen for this experiment.[55] There were two ways of evaluating the effective mass at each temperature, i.e. one was the susceptibility mass m_p^* deduced from the ω_p which was given by the horizontal intercept in the plot of n^2 vs ω^{-2} according to Eq. (22) in the absence of the external field and another was the cyclotron mass m_c evaluated from the split minima in the magneto-reflection. These experimental results are summarized in Table 4. According to Long[56] the direct energy gap, E_g, and the effective mass at the bottom of the conduction band, $m^*(0)$, have been given as follows:

$$E_g = 0.225\,\text{eV}, \quad m^*(0) = 0.0145\,m_0 \quad \text{at} \quad 77°\text{K},$$

$$E_g = 0.17\ \text{eV}, \quad m^*(0) = 0.0135\,m_0 \quad \text{at} \quad 300°\text{K}.$$

Here the effective mass values increase as the energy gap increases with decreasing temperature. Whereas in Table 4, the m_p^* decreases with decreasing temperature. This contradiction at a glance may be explained again in terms of the Kane's

Table 4. Mass parameters and dielectric constant deduced from the magneto-plasma reflectivity. The electron densities at 77°K and 300°K were $1.2\times10^{18}\text{cm}^{-3}$ for Sample A and $4.5\times10^{18}\text{cm}^{-3}$ for Sample B, respectively.

	Sample A			Sample B	
Temp. °K	m_p^*	m_c^*	ε_∞	m_p^*	ε_∞
300	$3.92\times10^{-2}m_0$	$4.18\times10^{-2}m_0$	15.5	$5.32\times10^{-2}m_0$	13.2
276	3.85 〃		15.5		
203	3.76 〃		15.4		
90	3.50 〃	3.72 〃	15.4		

m_p^*; Susceptibility mass obtained from the reflectivity minimum in the absence of the magnetic field,

m_c^*; cyclotron mass obtained from the magneto-plasma splitting in the field of 38.5 kgauss.

ε_∞; the dielectric constant in the high frequency limit.

(54) Made by the Princeton Appl. Res. Corp., Box 565, Princeton, New Jersey, U.S.A.

(55) InSb samples were purchased from the Consolidated Mining and Smelting Co. of Canada, Ltd. Dorchester Boulevard West, Montreal, 2, Canada.

(56) D. Long, J. Appl. Phys., **33** (1962), 1682.

theory[18),(52)] which gives the effective mass $m^*(N)$♯ for the electron concentration N as,[57]

$$m^*(N) = m^*(0)\left[1 + \frac{1}{2}\left(\frac{3}{\pi}\right)^{2/3}\frac{h^2 N^{2/3}}{E_g m^*(0)}\right]^{1/2}. \tag{31}$$

According to Eq. (31) the m^* for the sample A is estimated to be,

$$m^* = 0.0355\, m_0 \qquad \text{at} \quad 77°\text{K},$$

$$m^* = 0.0384\, m_0 \qquad \text{at} \quad 300°\text{K},$$

which seems to give the same temperature dependence as the observed m_p^*.

There are two possible explanations for the quantitative discrepancies between m_s^* and m_c^* of sample A.

(1) The m_p^* is the effective mass measured in the absence of the external field, whereas m_c^* is the effective mass in the presence of rather strong field.†) Since the conduction band of InSb is strongly non-parabolic, the effective mass value is dependent on the external field.

(2) If the electron in a plasma interacts with the phonon, the magneto-plasma splitting is influenced by the dispersion due to the lattice vibrations.[58] The vibration wavelength of InSb is 55μ and the 10% difference between m_p^* and m_c^* may be expected for an ideal model of parabolic energy surface.

It would be highly desirable to perform the magneto-plasma measurement with the sample of smaller electron concentration in which the plasma frequency becomes close to the frequency of lattice vibration.

3,5) Far-infrared absorption in $(HgTe)_{1-x}(CdTe)_x$

As it was mentioned in the previous section, the interaction between carriers in plasma and phonons would be an important factor of consideration on the dispersion characteristics of semiconducting compounds in the far-infrared wavelength region. Here the compound $(HgTe)_{1-x}(CdTe)_x$ was chosen for its infrared studies for the following reasons:

(1) HgTe has been found to give the semimetallic behavior in its transport properties,[59] whereas CdTe is a typical example of semiconductor with an energy gap of about 1.5 eV. Since the lattice parameter of the HgTe (6.4616 Å) is very close to that of CdTe (6.4816 Å), their ternary compounds may be made over the wide range of x. This allows us to investigate the optical and transport properties of the semiconductor-semimetal transition with the change in x.

♯) $m_c^* = m_p^* = m^*(N)$, since the conduction band in InSb is spherically symmetric.

(57) J. Kołodziejczak, Acta Phys. Polonica **20** (1961) 289.

†) The Landau spacing $\hbar\omega_c$ at the field of 40 kgauss is about 1.2×10^{-2} eV for $m^* = 0.038\, m_0$.

(58) I. Yokota, Private Communication. Also see, for the zero-field limit, J. Phys. Soc. Japan, **16** (1961), 2075.

(59) A.J. Strauss, T.C. Harman, J.G. Mavroides, D.H. Dickey and M.S. Dresselhaus, "Proc. International Conf. on Phys. of Semiconductors, Exeter 1962." Inst of Phys. and Phys. Soc., London, 1962, p. 703.

For the value of x near the semimetal-semiconductor transition point, the transport and optical properties of the ternary compound will be influenced strongly by the application of an external magnetic field.

(2) Although the transport properties of HgTe have allowed some investigators to conclude that it is a semimetal,[59),(60),(61),(62),(63] there are some other investigations[64),(65] in which it is regarded as a semiconductor with an energy gap in the neighborhood of 0.02 eV. In order that this ambiguity may be clarified the optical and magneto-optical measurement on HgTe-CdTe compounds in the far-infrared wavelength is highly desirable.

In the far-infrared measurements by Yamamoto et al.,[10] the compounds $(HgTe)_{1-x}(CdTe)_x$ for $x=0$, 0.15 and 1.00 were studied in the wavelength range from 25μ to 220μ at 310°K and 190°K. The original ingots of HgTe and CdTe were grown by the Bridgman's technique. The original constituent elements of HgTe were mixed in a quartz crucible and melted at 720°C for 30 hours. Similarly those of CdTe were treated at 1080°C for 60 hours. The temperature dependence of the Hall coefficient of HgTe showed an intrinsic behavior above 220°K, but the sample was p-type below 58°K. For preparation of $(HgTe)_{0.85}$ $(CdTe)_{0.15}$, both mother compounds were mixed in a form of powder in a quartz crucible and were melted at 800°C for 13 hours. The Hall coefficient of this compound was found negative (n-type) above 14°K. All of the above compounds were prepared in single crystals. The far-infrared spectrometer JASCO Model 501G[66] was used in a single beam operation with a Golay detector cell. The resolution of the over-all system, $\lambda/\Delta\lambda$, was 50 to 100 in our range of wavelength. Since the optical arrangement of this spectrometer required a large sample area (about 3 cm×6 cm), the material to be used for our measurement was ground in a form of powder. This powder was suspended in ethyl alcohol solution. Then finer grains of the specimen could be obtained by skimming over the surface of the liquid, and they were mixed with a molten paraffin and pasted on a plate of polyethylene about 1mm in thickness. With such preparation of specimen, it seemed natural to raise the question whether the measurements on the powder sample would give the same information as those on the bulk. The sample of CdTe was used to answer this question. The lattice vibration frequency of CdTe has been

(60) T. C. Harman, W.H. Kleiner, A.J. Strauss, G.B. Wright, J.G. Mavroides, J.M. Honig and D.H. Dickey, Solid State Communications, **2** (1964), 305.
(61) H. Rodot, M. Rodot and R. Triboulet, Comptes Rendus, **255** (1963), 5535.
(62) W. Giriat, Z. Dziuba, R.R. Galazka, L. Sosnowski and T. Zarkzewski, "Proc. International Conf. on Phys. of Semiconductors, Paris, 1964", (Dunod, Paris, 1964), p. 1251.
(63) R.N. Brown and S. Groves, Bull. Amer. Phys. Soc. Ser. II, **11** (1966), p. 206.
(64) A.D. Shneider and I.V. Gavrishchak, Fizika, Tverdogo Tela, **5** (1963), 1208, English Translation in Sov. Phys. -Solid State, **5** (1963), 881.
(65) M.D. Blue, Phys. Rev., **134** (1964), A226; also "Proc. International Conf. on Phys. Semiconductors, Paris 1964", (Dunod, Paris, 1964), p. 233.
(66) The Japan Spectroscopic Co., Ltd., Kitahachioji, Hachioji, Tokyo.

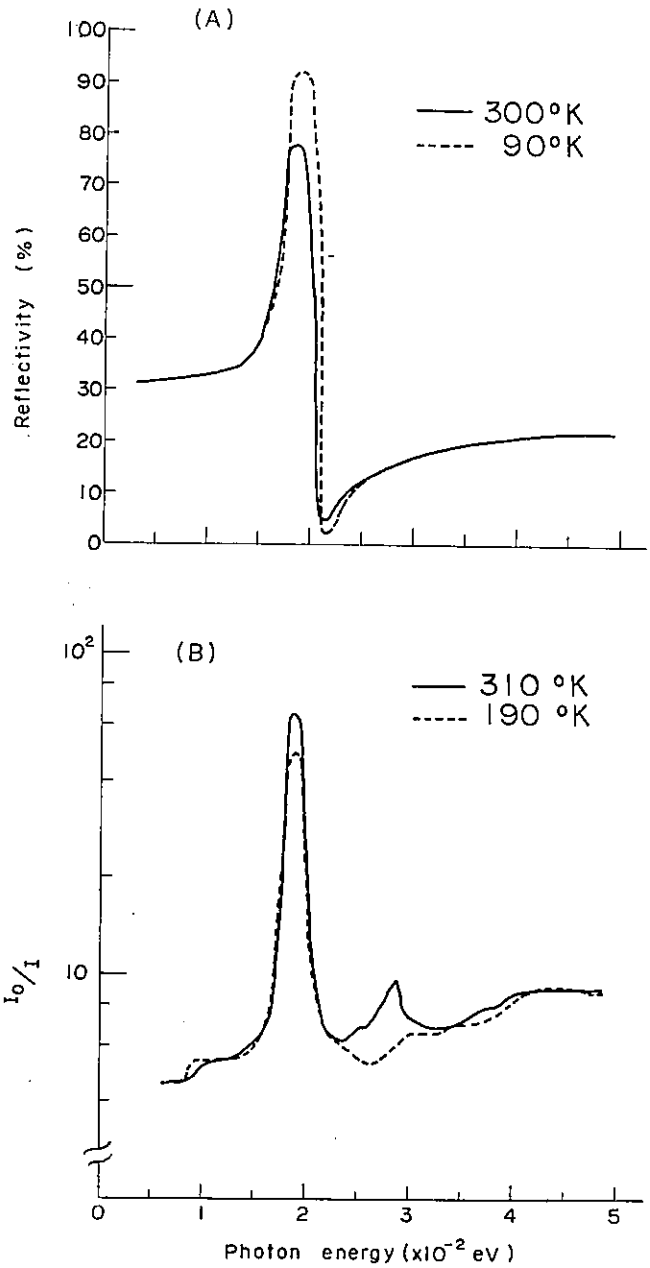

Fig. 9. The far-infrared spectra in CdTe,
(A) The reflectivity of bulk sample at 90°K and 300°K[67]
(B) The absorption of the powdered sample at 190°K and 310°K.
I_0/I: ratio of the spectrometer signal output without sample to that with sample.

(67) A. Mitsuishi, J. Phys. Soc. Japan, **16** (1961), 533.

measured by Mitsuishi[67] in terms of the reflectivity on the bulk sample. It was found to be 1.85×10^{-2}eV ($67.0\,\mu$) at 300°K and 1.91×10^{-2} eV (65.0μ) at 90°K as shown in the Fig. 9(A). The present measurements also gave the absorption peak at 1.88×10^{-2} eV (66.0μ) at 310°K and 1.90×10^{-2} eV (65.3μ) at 190°K in good agreement with the results of the measurements on the bulk as shown in Fig. 9(B). Thus the measurements on the powder could be assumed to give the same characteristics of its absorption spectrum as those of the bulk.

The absorption spectra for HgTe and $(HgTe)_{0.85}$ $(CdTe)_{0.15}$ at 310°K and 190°K are given in Figs. 10(A) and 10(B), respectively. For qualitative interpretation of these results, it would be worth-while to estimate the lattice vibration frequencies of these samples. In Fig. 11 the photon energies for the lattice vibration frequencies of various II-VI compounds observed by Mitsuishi et al.[68] are plotted against the inverse square root of the reduced mass of the constituent atoms. The straight line in the figure indicates that the photon energy, E_R, for the lattice vibration frequency is simply related to the reduced mass μ by

$$E_R \propto \sqrt{\frac{1}{\mu}}, \tag{32}$$

so that the force constant between the different neighboring atoms are nearly the same throughout the whole group of these compounds. If this observation also holds for our compounds the lattice vibration frequencies should be considerably lower than those for the observed peaks as shown by the energy E_R in Figs. 10 (A) and 10(B). The low temperature absorption data show only a minor structure at E_R for each sample. In addition, the energy for the absorption peak in Fig. 10(A) is quite dependent on the temperature unlike the characteristic of the lattice vibration. The reflectivity measurement on single crystal of HgTe by Dickey and Mavroides[69] has given the photon energy for lattice vibration as 1.43×10^{-2} eV ($87\,\mu$). In view of these facts, the major peaks in Fig. 10 (A) have to be attributed to physical reasons other than lattice vibration.

The tentative explanation for the spectra of HgTe in Fig. 10(A) may be given in terms of the plasma resonance with both electrons and holes with the following parameters:

Electron concentration:

$N_e = 1.80\times10^{17}\,\mathrm{cm}^{-3}$ at 310°K

$= 3.20\times10^{16}\,\mathrm{cm}^{-3}$ at 190°K.

Hole concentration:

$N_h = 1.70\times10^{18}\,\mathrm{cm}^{-3}$ at 310°K

$= 1.55\times10^{18}\,\mathrm{cm}^{-3}$ at 190°K.

(68) A. Mitsuishi, H. Yoshinaga and S. Fujita, J. Phys. Soc. Japan, **13** (1958), 1235.
(69) D.H. Dickey and J.G. Mavroides, Solid State Communications, **2** (1964), 213.

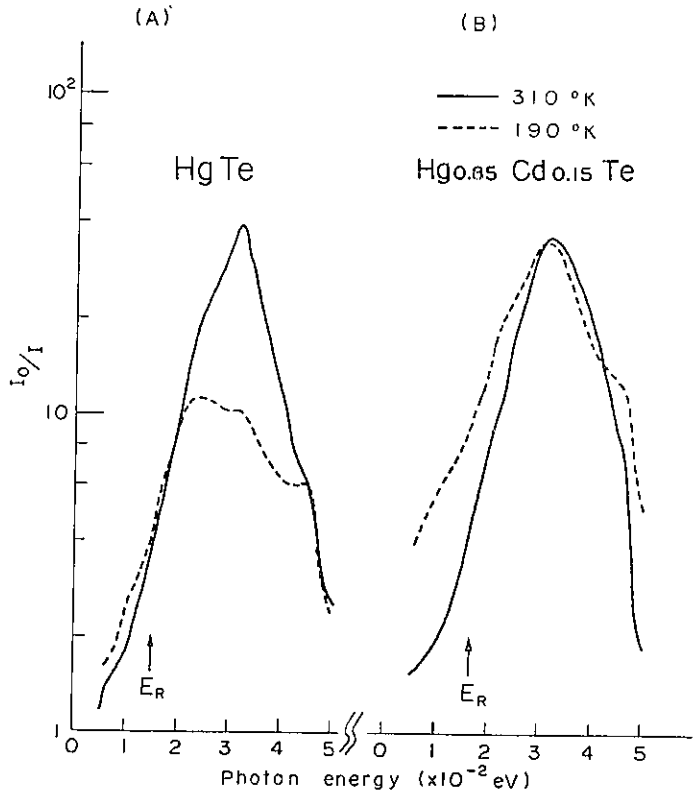

Fig. 10. The far-infrared absorption in the powder samples of (A) HgTe and (B) $(HgTe)_{0.85}$ $(CdTe)_{1.00}$ at 300°K and 190°K.

Electron effective mass: $m_e = 0.03\, m_0$ [19]

Hole effective mass: $m_h = 0.3\, m_0$ [70]

Mobility ratio: $b \equiv \dfrac{\mu_e^*}{\mu_h^*} = 41$

Dielectric const.[19]: $\varepsilon = 15$.

Here the plasma resonance frequency, ω_p, for the mixture of both carriers is given by

$$\omega_p^2 = \omega_{pe}^2 + \omega_{ph}^2, \tag{33}$$

where the ω_{pe}, ω_{ph} are the plasma frequencies for the electron and the hole alone, respectively. The concentrations and the mobility ratio for these carriers were obtained from the temperature dependence of the Hall coefficient[71] with the assumption of a two band model. Hence the evaluated values of $\hbar\omega_p$ are

$$\hbar\omega_p = 3.27 \times 10^{-2}\ \text{eV}\ (37.9\,\mu) \qquad \text{at} \quad 310°\text{K},$$

(70) E. Cruceanu, D. Niculescu, N. Nister, I. Stamatescu and S. Ionescu-Bujor, Sov. Phys.-Solid State, **7** (1965), 1456.

(71) M. Yamamoto, to be published.

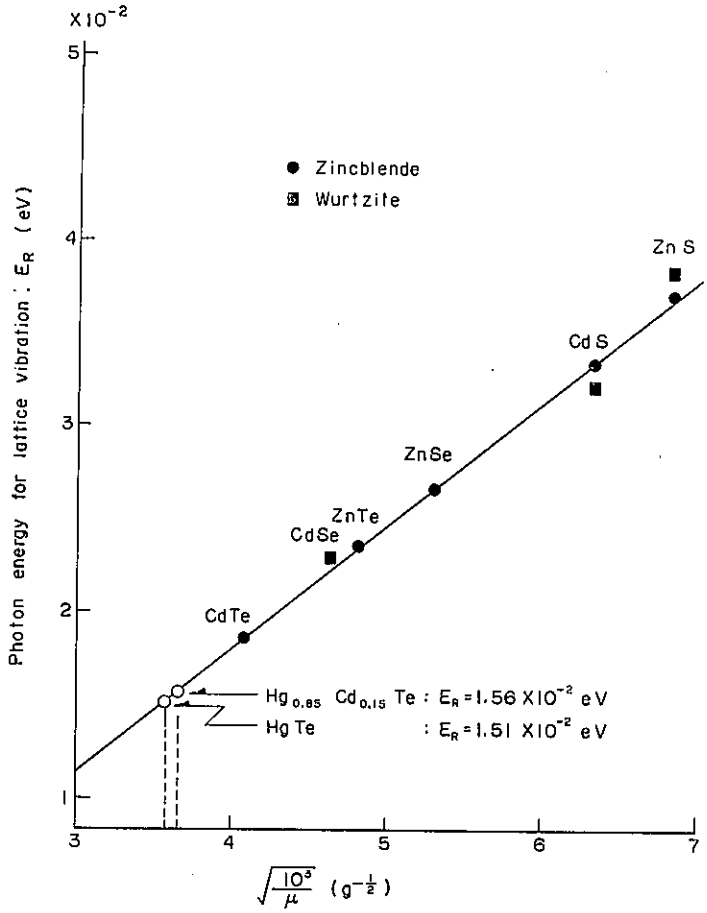

Fig. 11. The plot of lattice vibration frequencies in II-VI compounds vs. the inverse square root of the reduced masses of the constituent atoms, μ. The extrapolation of the straight line predicts the photon energies (E_R) for vibration frequencies in HgTe and $Hg_{0.85}$ $Cd_{0.15}$ Te.

and $$\hbar\omega_p = 2.39 \times 10^{-2}\,\text{eV}\,(51.9\,\mu) \qquad \text{at} \quad 190°\text{K},$$

which correspond to the major peak at 310°K and its shift to the lower photon energy at 190°K in Fig. 10(A).

At present the explanation for the spectra for $(HgTe)_{0.85}$ $(CdTe)_{0.15}$ have not been made yet with reasonable plausibility. The major peak in Fig. 10(B) is quite temperature independent. It is unlikely that the peak is related to a plasma resonance. The carrier concentrations evaluated from the Hall coefficient are

Electrons: $N_e = 7.90 \times 10^{17}\,\text{cm}^{-3}$ at 310°K

$= 4.56 \times 10^{17}\,\text{cm}^{-3}$ at 190°K,

Holes: $N_h = 1.41 \times 10^{19}\,\text{cm}^{-3}$ at 310°K

$= 1.38 \times 10^{19}\,\text{cm}^{-3}$ at 190°K,

with their effective masses[72]

$$\text{Electrons:} \quad m_e = 0.015\, m_0,$$

$$\text{Holes:} \quad m_h = 0.30\, m_0.$$

With these parameters, the photon energy for the plasma resonance frequency, $\hbar\omega_p$, is found to be

$$\hbar\omega_p = 9.55 \times 10^{-2}\,\text{eV}\,(13.0\,\mu) \quad \text{at} \quad 310°\text{K}$$

$$= 8.35 \times 10^{-2}\,\text{eV}\,(14.9\,\mu) \quad \text{at} \quad 190°\text{K},$$

so that they should lie outside of our wavelength region.

Since the measurements on the powder tend to be restricted by the line broadening of the absorption, it would be better to investigate the optical properties by reflection on the bulk, and more preferably with the magnetic field in various configurations.

3,6) Lattice vibrations in GaSe and GaS

Another far-infrared measurement on the lattice vibration was made by Kuroda et al.[73] on GaSe and GaS at room temperature. The samples of GaSe were grown in quartz crucible by means of the Bridgman's technique. The thin pieces of the single crystal, cleaved from the original ingot had the thickness of 2.2, 3.2, 5.3 and 7.6μ (accuracy $\pm 0.2\ \mu$). Similarly GaS[74] sample, was 20μ thick. The far-infrared radiation was incident along the c-axis of the crystal. Fig. 12 shows a typical example of the absorption spectra for GaSe (2.2μ thick) and for GaS measured with the Model 501G spectrometer.[66] The strong absorption peaks were observed at 0.0264 eV (47.0 μ) for GaSe, and in the vicinity of 0.03388 (32μ) for GaS. Both of these absorption peaks are considered to be associated with the Γ(TO) mode of lattice vibration which is optically active in the infrared region. If only the nearest neighbor interaction between the constituent atoms is assumed to be important, the frequency, ω_R, of the Γ(TO) mode of the harmonic lattice vibration is given by

$$\omega_R = \sqrt{\frac{3f}{2\mu}},$$

where f and μ are the force constant and the reduced mass of the nearest pair of the different kind of atoms, respectively. Since μ (GaSe)=37.0 (molecular weight) and μ (GaS)=22.0, the above results of ω_R give:

(72) T.C. Harman, A.J. Strauss, D.H. Dickey, M.S. Dresselhaus, G.B. Wright and J.G. Mavroides, Phys. Rev. Letters, **7** (1961), 403.

(73) N. Kuroda, Y. Nishina, T. Fukuroi and H. Baba, Bull. Phys. Soc. Japan, (Tokyo, 1966) **4**, p. 69, (in Japanese).

(74) Provided by the Dr. E. Mooser of the Cyanamid European Research Inst.

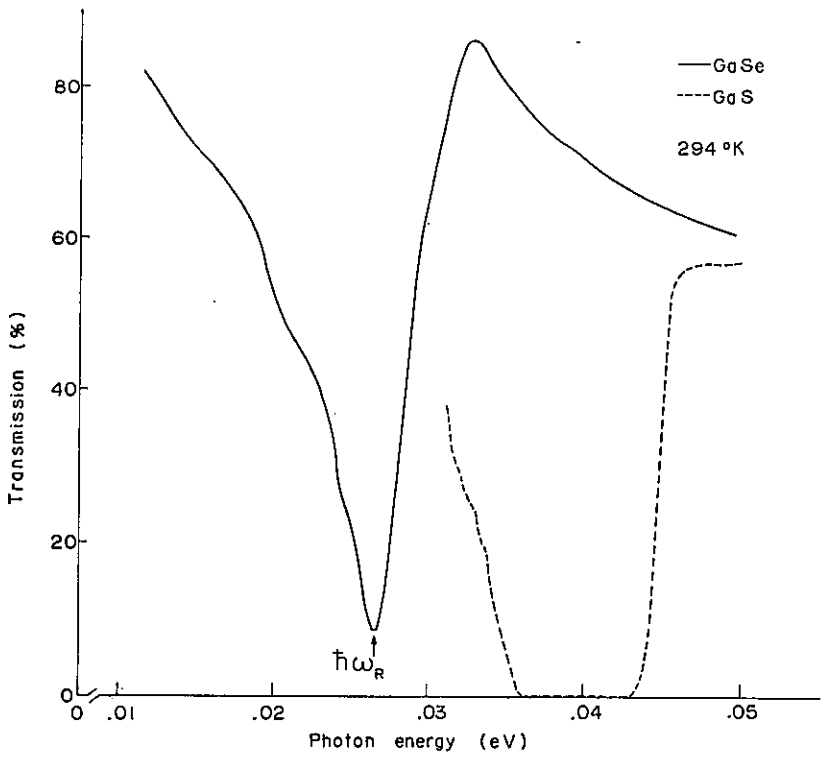

Fig. 12. The far-infrared absorption spectra of GaSe (2.2μ thick) and GaS (20μ thick) at 294°K.

$$f(\mathrm{GaS})\,/\,f(\mathrm{GaSe}) = 1.3$$

$$\text{with } f(\mathrm{GaSe}) = 6.57 \times 10^4 \text{ dyne cm}^{-1}.$$

This figure implies that the coupling of the Ga-S pair is stronger than that of Ga-Se. The observed values of ω_R show appreciable quantitative discrepancies when compared with the experimental results of Leung et al.[75] The reason for such disagreement is left for further investigation.

Summary

The energy levels, the effective mass and the effective g-factor are the fundamental parameters in describing the electronic band structures of semiconductors. These quantities for the groups II-IV, III-VI, III-V, II-VI compounds and Ge have been measured in terms of their absorption and the rotatory dispersion. Each of the above materials was studied with particular reference to the following problems:

(75) D.C. Leung, G. Andermann and W.G. Spitzer and C.A. Mead, J. Phys. Chem. Solids, **27** (1966), 849.

(1) The rotatory dispersion associated with exciton formation in Ge, and the effect of strain on the degenerate band.
(2) The band structures of layer type crystal structure in GaSe.
(3) The ellipsoidal and non-parabolic band structures in PbTe and PbSe.
(4) The magneto-plasma properties of electron and its possible interaction with phonons in InSb.
(5) The band structure of $(HgTe)_{1-x}$ $(CdTe)_x$ with particular interest in the verification of almost-zero-energy gap.

The non-parabolicity of the band structure has to be taken into account for explaining the dependence of the effective masses on the carrier concentration in PbTe and PbSe possibly in terms of the Cohen's model and in the case of InSb with the k·p approximation by Kane.

The current problems of interest lie in the optical anomalies which may not be explained in terms of one electron approximation. The optical anomaly associated with the exciton has been recognized as an example of the problems of this nature. In this connection the analytical solution for the exciton in a two dimensional crystal in a magnetic field could be used for understanding qualitatively the results on the magneto-optical measurement in GaSe. The absorption spectra caused by the lattice vibrations in HgTe and GaSe propose interesting problems in connection with their crystal structures and with the interaction of carriers in plasma with phonons. It is also expected that our knowledge on the lattice vibration frequencies would provide the information on the temperature dependence of the mobility.

Acknowledgments

This research project was supported in part by the Grand-in-Aid for Institutional Research (1965, 1966), by the Grand-in-Aid for Cooperative Research (from 1964 to 1966) from the Ministry of Education, by the Grant from the RCA Res. Labs., Tokyo (1963), and from the Matsunaga Science Foundation (1964). The early stage of our work on GaSe was performed as a cooperative research project in the Inst. for Solid State Phys., Tokyo Univ. It is our pleasure to thank Prof. T. Sakurai and Dr. S. Takahashi of the Res. Inst. for Scientific Measurements for their valuable information on some of the spectroscopic techniques quoted in Sec. 3.3. The PbSe sample was provided by Dr. N. Ohashi through the kind arrangement of Prof. K. Igaki in the Faculty of Engineering. We are also indebted to Mr. T. Nakazawa for designing the optical arrangements referred to in Sec. 3.4.